Scientia Iranica D (2023) 30(5), 1703–1713

SCIENTIA IRANICA

Sharif University of Technology
Scientia Iranica
Transactions D: Computer Science & Engineering and Electrical Engineering
http://scientiairanica.sharif.edu

A frequency and polarization reconfigurable L-shaped patch antenna with defected ground structure

P. Rawal and S. Rawat*

Department of Electronics and Communication Engineering, Manipal University Jaipur, Rajasthan, India.

Received 8 March 2021; received in revised form 5 August 2021; accepted 29 November 2021

KEYWORDS
Reconfigurable antenna;
Polarization reconfigurable antenna;
Circular polarization;
PIN diode;
Frequency reconfiguration;
Defected ground structure;
Wide band.

Abstract. A novel geometry for an antenna with polarization and reconfigurable frequency is proposed in this paper. The proposed antenna consists of an L-shaped patch antenna whose arms are separated using PIN-diode. Two parasitic elements, shorted back element, and edge tapered defected ground structure with slot are used for achieving wide impedance and axial ratio bandwidth. The proposed antenna acts as a circular polarized antenna with an axial ratio band width of 1.183 GHz and impedance bandwidth of 3.09 GHz in the ON state of both diodes and serves as a linear polarized reconfigurable frequency antenna in the remaining states of diodes.

1. Introduction

In a wireless communication system, antenna plays a highly important role. In addition, the antenna performance is of high significance in the overall functioning of wireless systems. In the case of spacecraft, satellite, and aircraft where the low size, low weight, moderate cost, and ease of installation are the constraints, low-profile antennas like microstrip antennas can be used [1–3]. With the development of technology and design, the performance of antennas can also be improved. Reconfigurable antennas are great options for researchers because they are able to configure their characteristics according to the desired response, and all of the above-mentioned characteristics can be introduced to reconfigurable antennas. A single antenna replaces two or more antennas in order to achieve multiple goals [4]. In this respect, a number of techniques have been discussed and elaborated in the literature to date [4]–[24] to achieve the desired frequency, pattern, and polarization reconfigurability. Frequency and polarization reconfigurable antennas enjoy great advantages in antenna technology. A frequency and polarization reconfigurable antenna with multiband coverage can replace multiple antennas and reduce the total antenna size. Polarization reconfigurable antennas can mitigate the fading effect and increase the channel capacity [21], hence being widely used in frequency reuse [23]. Circular polarization gains significance in polarization given its capability to reduce multipath distortion or fading [25–27]. In addition, there is no need for precise alignment of transmitting and receiving antennas [25–27]. It can also mitigate the polarization mismatch [27,28], which makes it applicable to radars, RFIDs, satellite communication, sensor systems, and global navigation systems [29,30].

*. *Corresponding author.*
E-mail addresses: prawal87@gmail.com (P. Rawal); sanyog.rawat@jaipur.manipal.edu (S. Rawat)

doi: 10.24200/sci.2021.57874.5451

Many reported studies have employed different techniques to achieve reconfiguration. For instance, surface integrated waveguide and PIN diode as the control elements [10], cross aperture with RF switch [11], corner truncated perturbation, PIN diode and single feed [15], two feeds on the adjacent edges [16], monopole antenna with two conducting strips in the ground plane controlled by PIN diode [21], circular patch antenna fed at four different points and controlled using PIN diode [22], two orthogonal meandered monopole fed by Wilkinson power divider and phase shifter and controlled by PIN diode [23], four straight dipoles with six pairs of pin diodes [31], diagonally fed square patch with parasitic stubs and pin diode [32], and discontinuous ring dipole with pin diode [33] are used to achieve polarization reconfigurable antennas. Here, Refs. [13–16,19,20] are the frequency reconfigurable antennas in which the PIN diodes are used as the control elements to change the electrical length to achieve frequency reconfigurability.

The proposed antenna is an L-shaped planar patch antenna with defected ground plane and parasitic elements. Two PIN-diodes (Alpha's silicon planar beam lead PIN-diode DGS6474) are used between the arms to achieve reconfigurability.

2. Antenna design

The proposed reconfigurable antenna design, which is an L-shaped polarization and frequency reconfigurable antenna, is presented in Figure 1. The proposed prototype design is simulated using the CST-Microwave studio. Its structure is fabricated on the FR-4 dielectric substrate with a dielectric constant of 4.4 and loss tangent of 0.025. The overall dimension of the antenna is 42 mm × 35 mm × 1.59 mm. The proposed design comprises two orthogonal arms as patch, slotted Defected Ground Structure (DGS), two parasitic patches and two shorting pins with stubs, two PIN-diodes, and three 47 nH inductors for RF choke. The length of the

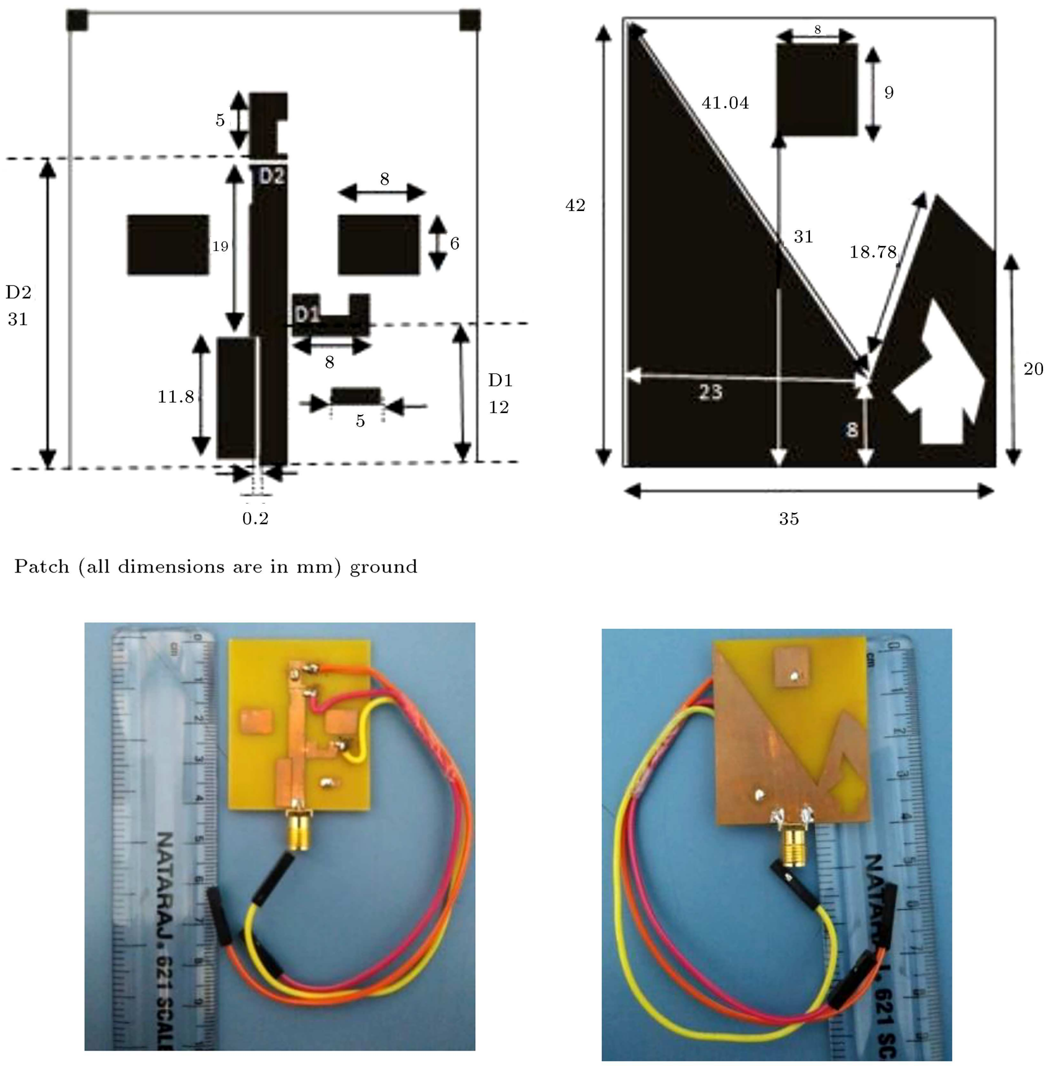

Figure 1. Simulated and fabricated design.

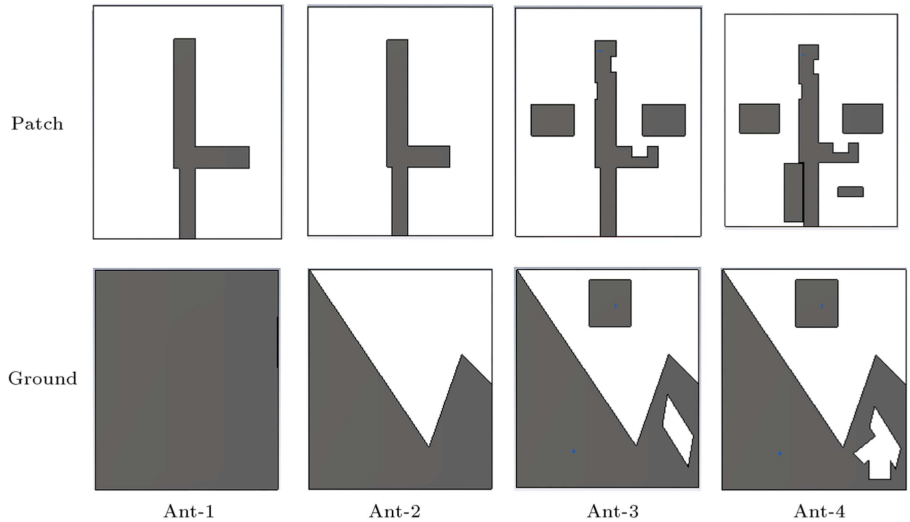

Figure 2. Design evolution steps.

vertical arm is 20 mm, which is nearly equal to $\lambda/2$ of the lower frequency (5.612 GHz) of the operating band (5.612 to 8.702 GHz), where λ is the effective wavelength. The horizontal arm is 8 mm long, which is nearly equal to $\lambda/2$ of the higher frequency (8.702 GHz) of the operating band. The defected ground plane is applied to achieve circular polarization and wide bandwidth. Two rectangular parasitic patches and two shorting pins with stub are also utilized to enhance the bandwidth. The antenna in this study is fed by the microstrip line of 50 Ω characteristic impedance with optimized dimensions. A coupled microstrip is then used to improve the impedance matching. Two PIN diodes (DGS6474) are connected to achieve frequency and polarization reconfigurability. Diode 1 (D1) is connected at the interface point between the horizontal arm and feed line, and Diode 2 (D2) is connected at a less than 5 mm distance from the top edge of the vertical arm.

Figure 2 shows the design evolution steps using four iterations called Ant-1, Ant-2, Ant-3, and Ant-4. Ant-1 has an L-shaped patch with full ground plane; Ant-2 has an L-shaped patch with reduced horizontal arm length and edge tapered DGS; Ant-3 is designed based on the introduction of parasitic patches and shorted elements in Ant-2; Ant-4 has slotted DGS and modified coupled stripline and L-shaped patch.

3. Impedance and axial ratio bandwidth enhancement and empirical formulas

Ant-1 is a linearly polarized dual band (4.73 GHz and 10.25 GHz) antenna with 100 MHz and 1.27 GHz Impedance Bandwidths (IBW). The vertical arm is responsible for 4.73 GHz resonance frequency, while the horizontal arm is responsible for 10.25 GHz resonance frequency. The lengths of vertical (l_v) and horizontal (l_h) arms are approximately half of the wavelength of resonance frequencies. The length of the antenna is calculated approximately using Eqs. (1) and (2) [1–3]:

$$l_0 \cong \frac{\lambda_0}{2} \cong \frac{\lambda_r}{2\sqrt{\varepsilon_{reff}}} \cong \frac{c}{2f_r\sqrt{\varepsilon_{reff}}}, \tag{1}$$

where c is the light speed, λ_0 the free space wavelength, f_r the resonance frequency, and ε_{reff} the approximate effective dielectric constant:

$$\varepsilon_{reff} \cong \frac{\varepsilon_r+1}{2} + \frac{\varepsilon_r-1}{2}\left[1+12\frac{h}{w}\right]^{-\frac{1}{2}}. \tag{2}$$

Two electric field vectors with equal magnitude and quadrature in phase (orthogonal modes) are required to produce circular polarization [34,35]. Of note, the dimensions of a finite ground plane have made a major contribution to edge diffraction for antenna radiation [36]. The defected ground can be used for improved bandwidth [37] and multiband operation [38,39]. Hence, in the case of Ant-2 structure, a DGS with the slope and patch dimensions is introduced so that it can produce circular polarization. Now, the antenna is circularly polarized with an Axial Ratio Bandwidth (ARBW) of 940 MHz (6.81 GHz to 7.75 GHz). Figure 3 shows the frequency shift in the resonance frequency due to coupling between the radiating magnetic currents and ground plane edges. Shifting in the resonance frequency is determined by Eq. (3) [36]:

$$\frac{\Delta f}{f} = -4\sqrt{\varepsilon_e}\frac{\Delta l_d}{\lambda_0}, \tag{3}$$

where Δl_d is the length extension due to diffraction. Here, two rectangular parasitic patch elements are placed in the reactive region in the vicinity of the vertical arm field. The distance of the reactive near field can be calculated using Eq. (4) [1]:

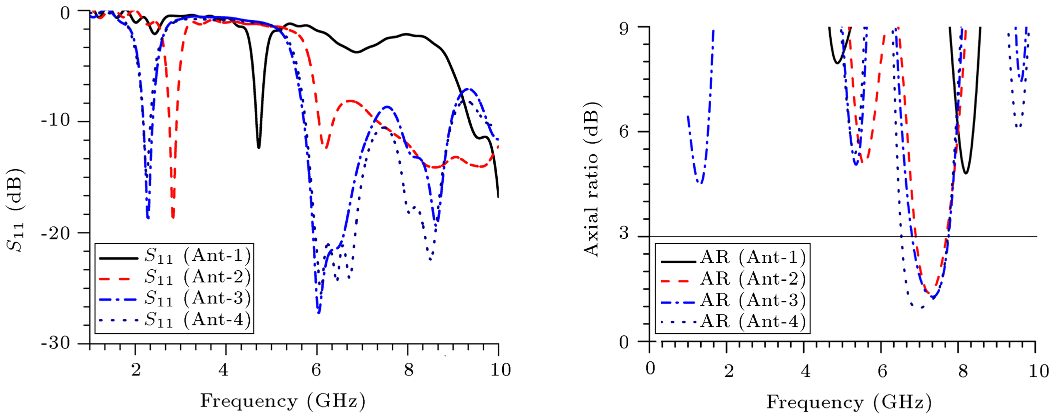

(a) (b)

Figure 3. (a) Reflection coefficient (S_{11}) variation for Ant-1, Ant-2, Ant-3, and Ant-4. (b) Axial ratio variation with frequency.

$$\textit{Reactive near field} \leq 0.62 \times \sqrt{\frac{l_v^3}{\lambda}}, \tag{4}$$

where l_v is the length of vertical arm. There is an air gap between the patch and parasitic element and for this reason, a fringing field is introduced and the antenna bandwidth is enhanced [37]. A rectangular element with a shorting pin on the bottom side is also introduced. The incorporation of shorting pins induces a shunt inductive effect [40,41], leading to an increase in the electrical length of the antenna. Reduction of the antenna size is achieved through shorting pin [42,43]. Some cuts are also introduced into the patch. Therefore, the addition of parasitic elements, shorting pins with back elements, cuts in the patch, and defected grounds have a combined effect that improves both the impedance and ARBW. A small rectangular stub and cut of the inverted λ shape are also introduced to improve the ARBW. A hump is further detected in the simulation result; therefore, a coupled microstrip line is introduced near the feed. Due to the presence of this coupled element, hump is removed and the values of the antenna impedance and ARBW reach 3.226 GHz and 1.435 GHz, respectively.

4. Parametric analysis of the proposed design

4.1. Effect of ground

The ground structure depicted in Figure 4 is responsible for circular polarization. A parametric analysis is done at the point y_1. Figure 5 shows the effect of this point on S_{11} and AR. Due to an increase in the value of y_1, the AR rises above 3 dB, followed by a dip in S_{11}; hence, a tradeoff point $y_1 = 8$ is selected. Simultaneously, point y_2 is introduced. As shown in Figure 6, S_{11} and AR are improved using y_2. The parametric results at point y_2 are shown in Figure 7 and the coordinates of point y_2 are finally chosen as (0, 20).

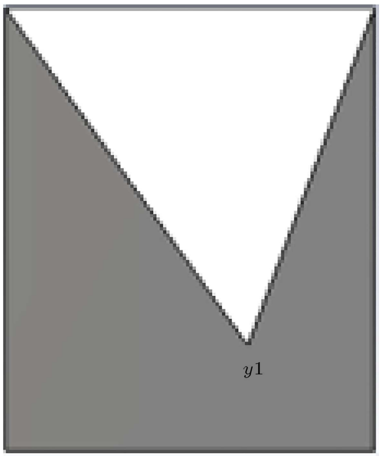

Figure 4. View of the edge-tapered ground (point y_1).

4.2. Effect of parasitic element

In Figure 8, two rectangular parasitic elements are introduced, and a parametric analysis is conducted on the patch dimension and the gaps between the patch and parasitic element. This analysis has a significant effect on S_{11}, as demonstrated in Figure 9. The dimensions of the parasitic elements are 8 mm × 6 mm and the gap is 4 mm. In this context, the antenna is a dual band antenna. At this point, AR is affected by the parasitic elements, as shown in Figure 9.

4.3. Effect of rectangular element on the back side and cut in patch

The electrical length increases using cuts applied to the patch and a rectangular element on the back side shorted with patch. The frequency response is shifted to the lower side, thus increasing the IBW. The ARBW also increases due to this combined effect. Parametric results are shown in Figure 10. It should be noted that the element length has major impact on AR and S_{11}.

4.4. Effect of coupled microstrip line near feed

At 7.5 GHz, an impedance mismatch causes a hump

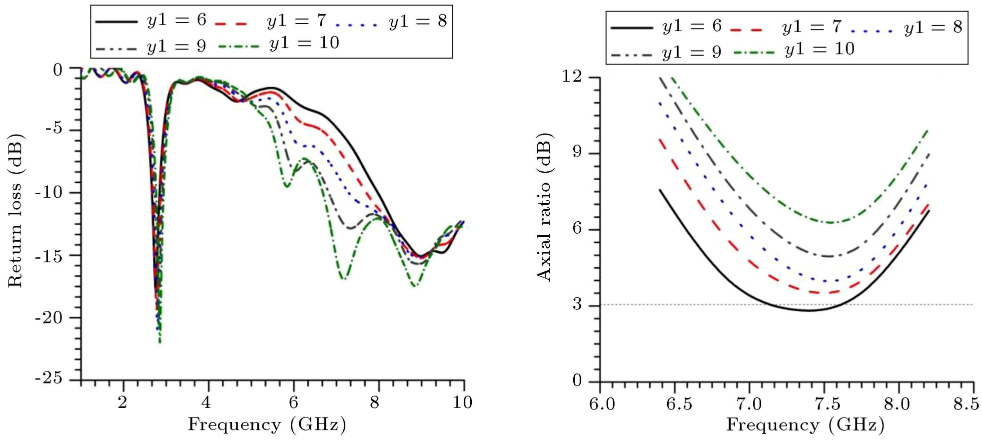

Figure 5. Effect of point y_1 on return loss and axial ratio.

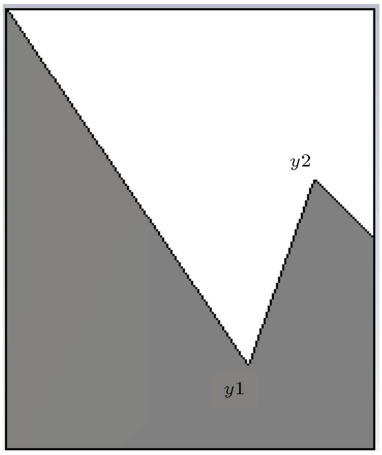

Figure 6. View of edge-tapered ground (points y_1 and y_2).

to appear in the S_{11} plot. A coupled microstrip line is introduced near the feed with the separation of 0.2 mm from the feed line. A capacitive effect occurs at the feed line and impedance is matched. Hence, a hump is removed and antenna radiates at 3.226 GHz band from 5.751 GHz to 8.977 GHz. Parametric analysis of the

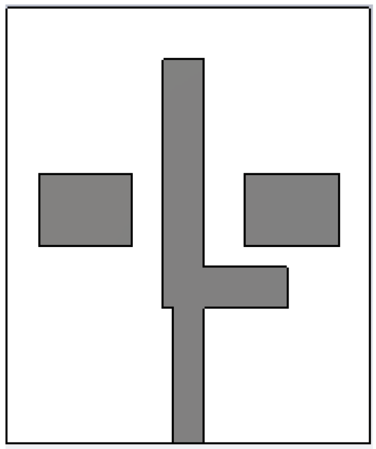

Figure 8. L-shaped patch with parasitic elements.

gap between the feed line and coupled microstrip line is shown in Figure 11, showing its key effect on S_{11}.

5. Result and discussion

The proposed antenna is fabricated on the FR 4 substrate with a height of 1.59 mm and loss tangent

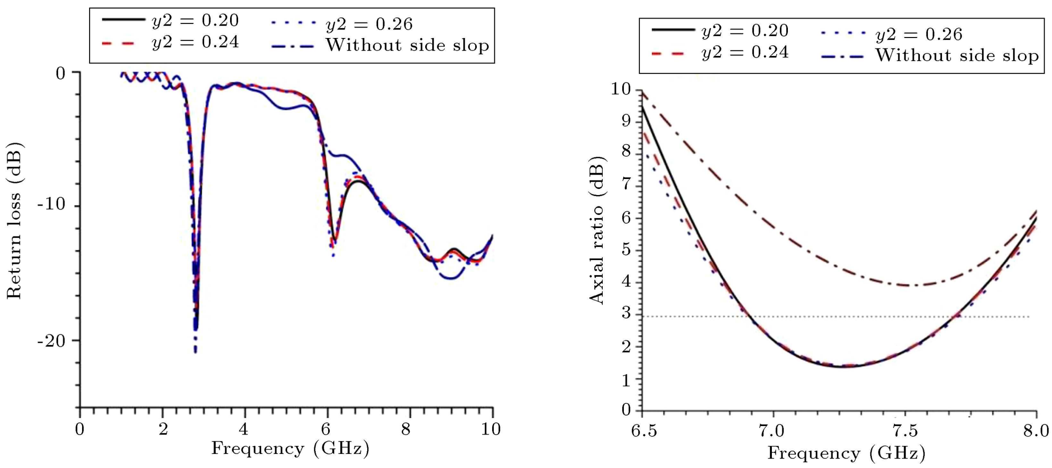

Figure 7. Effect of y_2 on return loss and axial ratio taking y_1 as constant.

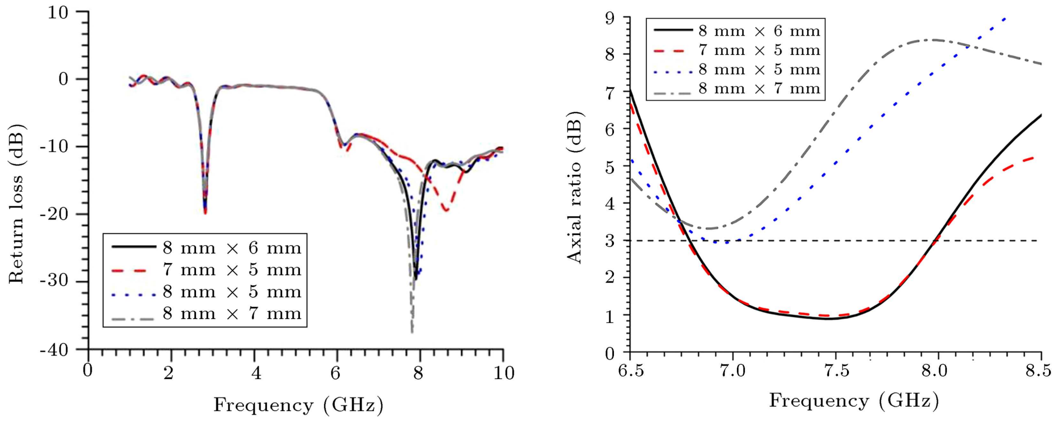

Figure 9. Effect of parasitic element on return loss (S_{11}) and axial ratio.

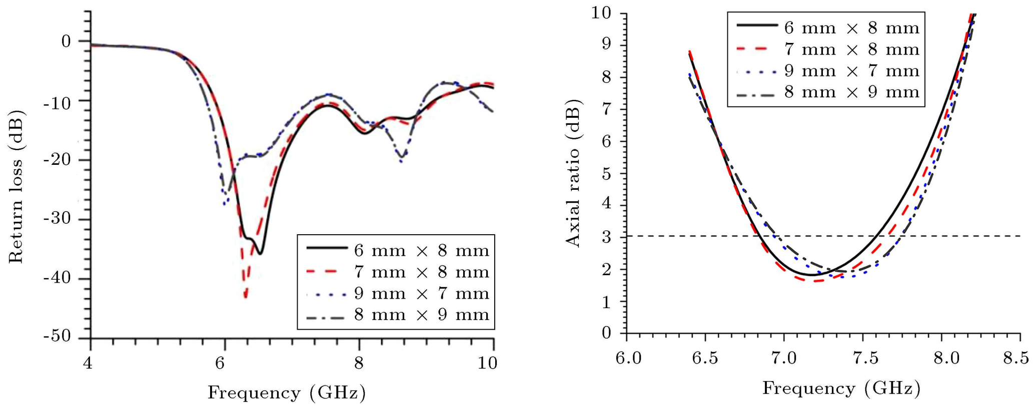

Figure 10. Effect of rectangular element and cuts on S_{11} and AR.

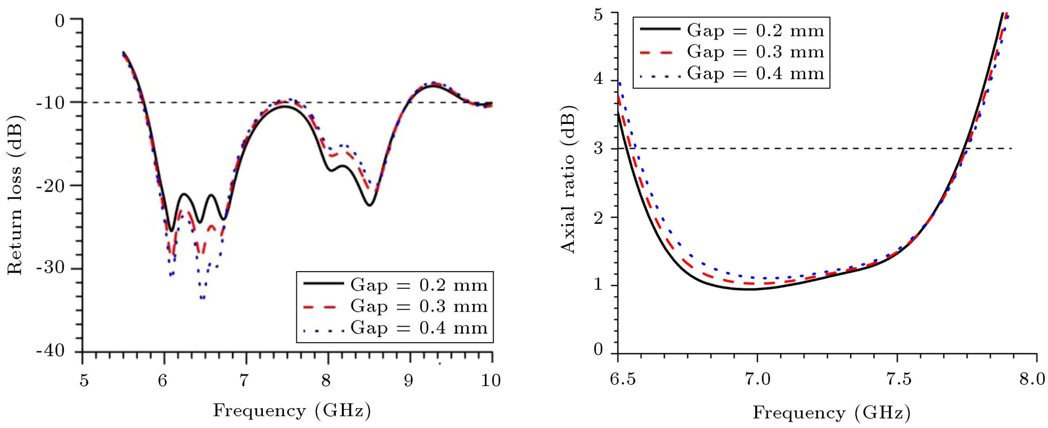

Figure 11. Effect of coupled microstrip line near feed on S_{11} and AR.

of 0.025. The design is simulated via the CST studio suite (V 2018) and measured on Anritsu VNA Master (Model: MS2028C/11). Figure 12 shows the simulated results of the return loss and AR.

As demonstrated by the simulated results, when the two diodes are on, we have a wideband circular polarized antenna with 43% (3.09 GHz, i.e., 5.612 to 8.702 GHz) IBW and 1.183 GHz (6.503 to 7.686 GHz) ARBW. In case diode D1 is on and D2 is off, the antenna becomes a linearly polarized dual band antenna at the center frequencies of 6.5 GHz and 9.3 GHz with the IBW of 5151 MHz and 951 MHz, respectively. When diode D1 is off and D2 is on, we have a wideband linearly polarized antenna with an IBW of 2671 MHz. In the last case, when both diodes are off, the antenna becomes a linearly polarized dual band antenna with the IBW of 2121 MHz and 523 MHz. Table 1 shows the IBW, ARBW, and type of polarization with different states of diodes. Figure 13 shows simulated and measured return losses in different

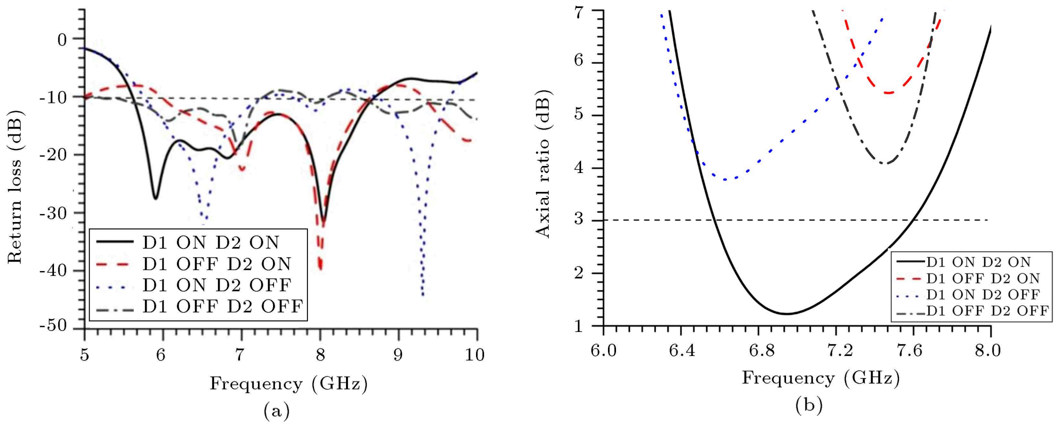

Figure 12. Simulated result (a) return loss and (b) Axial ratio.

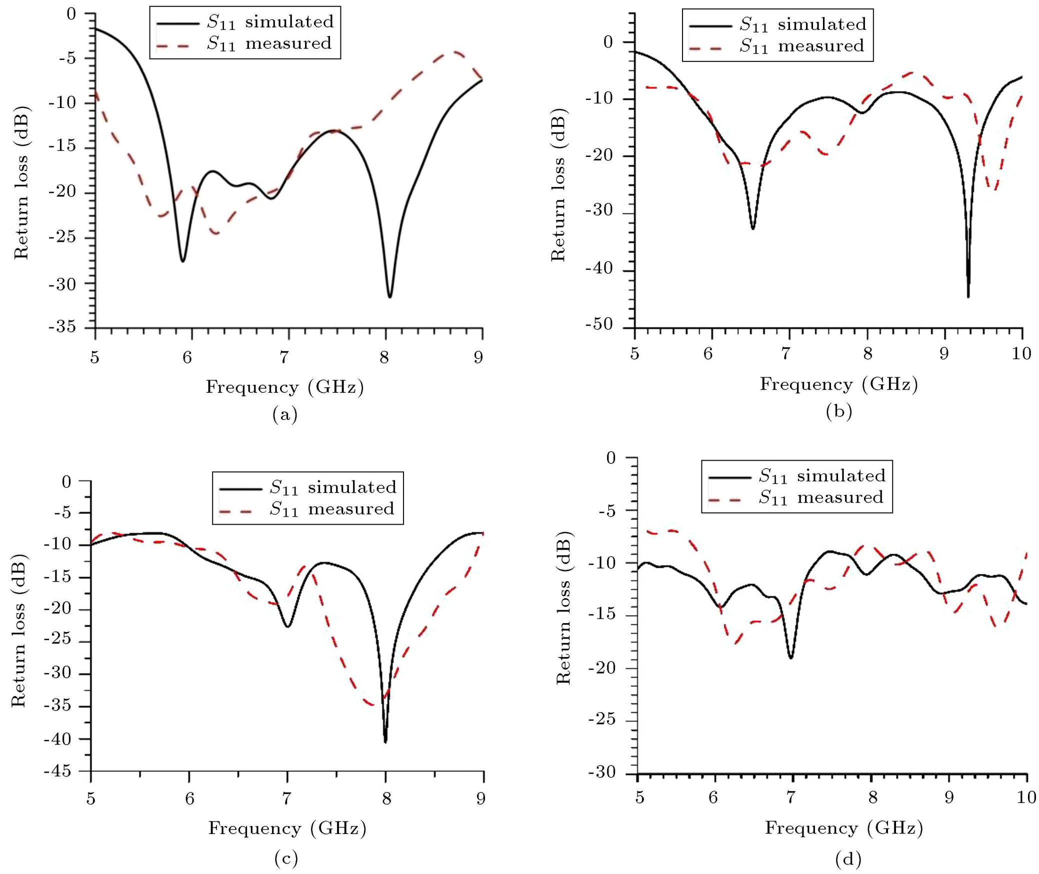

Figure 13. Simulated and measured result of return loss (a) Both diodes are ON, (b) D1 ON D2 OFF, (c) D1 OFF D2 ON, and (d) Both diodes OFF.

Table 1. Relation among diodes state, IBW, and ARBW for the proposed antenna.

Diode state					
D1	**D2**	**IBW MHz**	**ARBW**	**Polarization**	**Band**
On	On	3090	1183	CP	Wide band
On	Off	1551, 951	–	LP	Dual band
Off	On	2671	–	LP	Wide band
Off	Off	2121, 523	–	LP	Dual band

Table 2. Comparison of the reported antennas with the proposed design.

Ref.	Antenna size mm^3	IBW, MHz	ARBW, MHz	Reconfiguration
[10]	$50 \times 50 \times 1.57$	240	–	LP
		770	270	LHCP, RHCP
[13]	$50 \times 50 \times 0.8$	Dual band (93, 103)	–	LP
		Dual band (227, 103)	–	RHCP
		Dual band (204, 74)	–	LHCP
[14]	$50 \times 50 \times 3.2$	Dual band (210, 210)	–	VP
		Dual band (600, 230)	–	HP
		Dual band (700, 510)	120, 50	RHCP
		Dual band (660, 550)	90, 40	LHCP
[18]	$35.2 \times 67.5 \times 1.52$	1850	–	LP
		500	170	RHCP
		500	170	LHCP
[20]	$88 \times 67 \times 0.8$	580	410	CP
		250	–	LP
[28]	$90 \times 90 \times 26$	140	60	CP
		140	–	LP
[30]	$33 \times 14 \times 15$	1410	460	RHCP
		1410	460	LHCP
Proposed	$42 \times 35 \times 1.59$	3090	1183	CP
		Dual band (1551,951)	–	LP
		2671	–	LP
		Dual band (2121, 523)	–	LP

states of diodes. The measured results are in good agreement with simulated results. The measured IBW was found to be slightly shifted in comparison to the simulated results. This shift in frequency can be due to the effect of fabrication error, inductor, soldering material, etc. Figure 14 shows the measured co-polar and cross-polar E plane pattern at 6.84 GHz and 7.3 GHz when both diodes are on. The difference in the magnitude of co-polar and cross-polar pattern was less than 3 dB, indicating that the circular polarization was satisfactory at these frequencies. The simulated results confirmed the AR to be well below 3 dB at those frequencies. Table 2 provides a comparison between the proposed antenna design and previously reported antennas.

6. Conclusion

This study introduces a novel antenna design that offers wideband polarization and frequency reconfigurability. The antenna features an L-shaped patch, parasitic element, shorted back element, and an edge-tapered defected ground structure with slots. Reconfigurability was controlled using the ON-OFF states of two PIN diodes. The antenna enjoyed ability to reconfigure itself at four different frequency bands and two polarizations (LP and CP). The impedance and axial ratio bandwidths of the proposed antenna were 3.09 GHz (5.612 to 8.702 GHz) and 1.183 GHz (6.503 to 7.686 GHz), respectively, in the ON state of both diodes. The antenna under study was a linearly polarized one in the remaining states of diodes which can be used in C-band wireless applications like RADAR, satellite communication, etc.

Acknowledgement

Authors wish to deliver their sincere thanks to Central

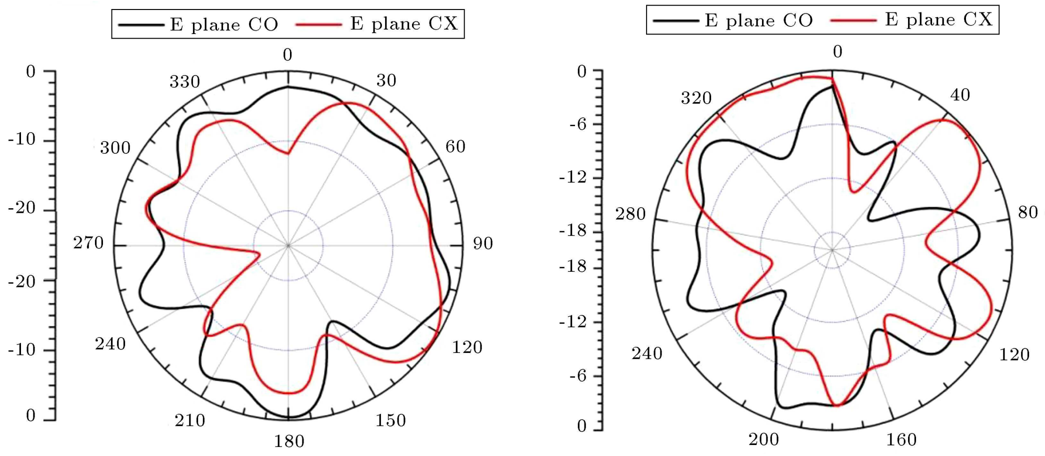

Figure 14. E plane pattern at (a) 6.84 GHz and (b) 7.3 GHz.

Research Facility (CRF) IIT Delhi for providing the measurement facilities.

References

1. Balanis, C.A., *Antenna Theory-Analysis and Design*, 3rd Edition, Wiley India, **170**, pp. 811–872 (2010).
2. Prasad, K.D., *Antenna and Wave Propagation*, 3rd Edition, Satya Prakashan, New Delhi, pp. 529–573 (2005).
3. Garg, R. and Bhartia, P., *Microstrip Antenna Design Handbook*, Artech House, pp. 1–28 (2001).
4. Haupt, R.L. and Lanagan, M. "Reconfigurable antennas", *IEEE Antennas and Propagation Magazine*, **55**(1), pp. 49–61 (2013).
5. Sedghara, A. and Atlasbaf, Z. "A novel single-feed reconfigurable antenna for polarizationand frequency diversity", *International Journal of Microwave and Wireless Technologies*, **9**, pp. 1–7 (2016).
6. Kakhki, M.B. and Rezaei, P. "Reconfigurable microstrip slot antenna with DGS for UWB applications", *International Journal of Microwave and Wireless Technologies*, **9**, pp. 1–6 (2017).
7. Nemati, N. and Bemani, M. "A novel reconfigurable microstrip fractal UWB antenna with six variable rejection frequency bands", *International Journal of Microwave and Wireless Technologies*, **12**, pp. 1–7 (2019).
8. Sulakshana, C. and Anjaneyulu, L. "Reconfigurable antennas with frequency, polarization,and pattern diversities for multi-radio wireless applications", *International Journal of Microwave and Wireless Technologies,*, **9**, pp. 1–12 (2015).
9. Cheng, Y.-F., Ding, X., Wang, B.-Z., et al. "An azimuth-pattern reconfigurable antenna with enhanced gain and front-to-back ratio", *IEEE Antennas and Wireless Propagation Letters*, **16**, pp. 1–4 (2017).
10. Hu, J., Hao, Z.-C., and Miao, Z.-W. "Design and implementation of a planar polarization-reconfigurable antenna", *IEEE Antennas and Wireless Propagation Letters*, **16**, pp. 1557–1560 (2017).
11. Lin, W. and Wong, H. "Polarization reconfigurable aperture fed patch antenna and array", *IEEE Access* , **4**, pp. 1510–1517 (2016).
12. Yang, K., Bao, X., and McEvoy, P. "Pattern reconfigurable back-to-back microstrip patch antenna", *IET Microwaves, Antennas & Propagation*, **10**(13), pp. 1390–1394 (2016).
13. Rawal, P. and Rawat, S. "A bowtie shaped frequency reconfigurable microstrip patch antenna with wide coverage area", *5th IEEE International Conference on Recent Advances and Innovations in Engineering (ICRAIE)* (2020). DOI: 10.1109/ICRAIE 51050.2020.9358341
14. Kumar, J., Basu, B., and Talukdar, F.A. "Modeling of a PIN diode RF switch for reconfigurable antenna application", *Scientia Iranica*, D, **26**(3), pp. 1714–1723 (2019). DOI: 10.24200/sci.2018.20110
15. Anantha, B., Merugu, L., and Rao, P.V.D.S. "A novel single feed frequency and polarization reconfigurable microstrip patch antenna", *Int. J. of Electronics and Communication (AEU)*, **72**, pp. 8–16 (2017).
16. Anantha, B., Merugu, L., and Rao, P.V.D.S. "A quad polarization and frequency reconfigurable square ring slot loaded microstrip patch antenna for WLAN application", *Int. J. of Electronics and Communication (AEU)*, **78**, pp. 15–23 (2017).
17. Faizal Ismail, M., Kamal M., Rahim, A., et al. "Dual band pattern reconfigurable antenna using electromagnetic band-gap structure", *International Journal of Electronics and Communications*, **130** (2020). DOI: https://doi.org /10.1016 /j.aeue.2020.153571
18. Cai, X., Wang, A., Ma, N., et al. "Novel radiation pattern reconfigurable antenna with six beam choices", *Science Direct (ELSEVIER)*, **19**(2), pp. 123–128 (2012).
19. Kishore, N., Prakash, A., and Tripathi, V.S. "A reconfigurable ultra-wide band antenna with defected

ground structure for ITS application", *Int. J. of Electronics and Communication (AEU)*, **72**, pp. 210–215 (2017).

20. Yadav, R. and Patel, P.N. "EBG inspired reconfigurable patch antenna for frequency diversity application", *Int. J. of Electronics and Communication (AEU)*, **76**, pp. 52–59 (2017).

21. Panahi, A., Bao, X.L., Yang, K., et al. "A simple polarization reconfigurable printed monopole antenna", *IEEE Transaction on Antenna and Propagation*, **63**(11), pp. 5129–5134 (2015).

22. Gu, H., Wang, J., and Ge, L. "A new quadric-polarization reconfigurable circular patch antenna", *IEEE Access*, **4**, pp. 4646–4651 (2016). DOI: 10.1109/ACCESS.2016.2600250

23. Cao, Y., Cheung, S.W., and Yuk, T.I. "A simple planar polarization reconfigurable monopole antenna for GNSS/PCS", *IEEE Transactions on Antennas and Propagation*, **63**(2), pp. 500–507 (2015).

24. Raman, S., Mohanan, P., Timmons, N., et al. "Microstrip-fed pattern and polarization reconfigurable compact truncated monopole antenna", *IEEE Antennas and Wireless Propagation Letters*, **12**, pp. 710–713 (2013).

25. Yektakhah, B. and Sarabandi, K. "A wide band circularly polarized omnidirectional antenna based on excitation of two orthogonal circular TE21 modes", *IEEE Transactions on Antennas and Propagation* (2017). DOI: 10.1109/TAP.2017.2714019

26. Ding, K., Gao, C., Qu, D., et al. "Compact broadband circularly polarized antenna with parasitic patches", *IEEE Transactions on Antennas and Propagation* (2017). DOI: 10.1109/TAP.2017.2723938

27. Tan, M.T. and Wang, B.Z. "A dual band circularly polarized planar monopole antenna for WLAN/WiFi application", *IEEE Antennas and Wireless Propagation Letters*, **15**, pp. 370–373 (2016).

28. Tran, H.H. and Park, I. "Wideband circularly polarized cavity backed asymmetric crossed bowtie dipole antenna", *IEEE Antennas and Wireless Propagation Letters*, **15**, pp. 358–361 (2016).

29. Wu, Z., Li, L., Li, Y., et al. "Metasurface superstrate antenna with wide band circular polarization for satellite communication application", *IEEE Antennas and Wireless Propagation Letters*, **15**, pp. 374–377 (2016).

30. Panahi, A., Bao, X.L., Ruvio, G., et al. "A printed triangular monopole with wideband circular polarization", *IEEE Transactions on Antennas and Propagation*, **63**(1), pp. 415–418 (2015).

31. Li, Q.Y., Tran, H.H., and Park, H.C., "Reconfigurable antenna with multiple linear and circular polarization diversity for WLAN applications", *Microw Opt Technol Lett*, pp. 1–7 (2018). https://doi.org/10.1002/mop.31411

32. Zhang, P.F., Liu, S.Z., and Zhao, S.A. "A novel reconfigurable microstrip patch antenna with frequency and polarization diversities", *Microw Opt Technol Lett.*, **57**(6), pp. 1494–1500 (2015).

33. Saraswat, K. and Harish, A.R. "Polarization reconfigurable discontinuous ring dipole antenna", *Microw Opt Technol Lett.*, **62**, pp. 1–8 (2019). https://doi.org/10.1002/mop.32015

34. Kumar, G. and Ray, K.P., *Broad Band Microstrip Antennas*, Boston, MA: Artech House (2003).

35. Kumar, R. and Chaudhary, R.K. "Compact asymmetric cross-shaped rectangular dielectric resonator antenna for wideband circular polarization", *Microw Opt Technol Lett.*, **61**, pp. 1–11 (2019). https://doi.org/10.1002/mop.31808.

36. Lier, E. and Jakobsen, K.R. "Rectangular microstrip patch antennas with infinite and finite ground plane dimensions", *IEEE Transactions on Antennas and Propagation*, **Ap-31**(6), pp. 978–984 (1983).

37. Gautam, A.K., Bisht, A., and Kanaujia, B.K. "A wideband antenna with defected ground plane for WLAN/WiMAX applications", *Int. J. of Electronics and Communication (AEU)*, **70**, pp. 354–358 (2016).

38. Prema, N. and Kumar, A. "Design of multiband microstrip patch antenna for C and X band", *Optik*, **127**, pp. 8812–8818 (2016).

39. Xia, Y.-Q., Chen, X.-R., and Tang, T. "A novel eight ports dual band antenna array for 2.4/3.5 GHz MIMO applications", *Optik*, **126**, pp. 1175–1180 (2015).

40. Patil, J.B. and Karia, D.C. "Design of circularly polarized microstrip patch antenna with inserting of shorting pins", *Proceedings of the 2nd International Conference on Inventive Communication and Computational Technologies (ICICCT) IEEE Xplore Compliant - Part Number: CFP18BAC-ART*; ISBN:978-1-5386-1974-2 (2018).

41. Zhang, X. and Zhu, L. "High-gain circularly polarized microstrip patch antenna with loading of shorting pins", *IEEE Transactions on Antennas and Propagation*, **64**, pp. 2172–2178 (2016). 10.1109/TAP.2016.2552544

42. Yoon, C., Choi, S.H., Lee, H.C., et al. "Small microstrip patch antennas with short-pin using a dual band operation", *Microwave Optical Technology Letters*, **50**(2), pp. 367–371 (2007). DOI: 10.1002/mop.23099

43. Saluja, N. and Khanna, R. "A novel extended edge-based compact PIFA antenna for mobile devices", *Optik*, **126**, pp. 1602–1605 (2015).

Biographies

Pallav Rawal received his BTech degree in Electronics and Communication engineering and MTech degree in Digital Communication in 2010 and 2014, respectively. Currently, he is pursuing PhD from Manipal

University Jaipur, Rajasthan, India and serving as an Assistant Professor at Swami Keshvanand Institute of Technology, M and G, Jaipur, Rajasthan, India. His research interests include reconfigurable antenna and smart antenna.

Sanyog Rawat is a highly experienced professional in the field of electronics and communication engineering, with over 17 years of teaching and research experience. He holds a Bachelor of Engineering degree in Electronics and Communication, a Master of Technology degree in Microwave Engineering, and a PhD in Planar Antennas. Dr. Rawat has published over 90 research papers in peer-reviewed international journals, book series, and IEEE/Springer conferences. He has also organized several workshops, seminars, national and international conferences. Dr. Rawat has supervised and guided numerous MTech and PhD students and has edited several books for Springer publication. His current research interests include reconfigurable RF printed circuits and passive and active microwave integrated circuits. Dr. Rawat serves as a reviewer for many Web of Science and Scopus indexed journals and is a member of several academic and professional bodies, including Fellow IETE and Life Member IE and ISLE. He has also traveled to several countries for academic and research purposes, including Japan, Thailand, Malaysia, UAE, and Indonesia.